www.czasopisma.pan.pl PAN POLSKA AKADEMIA NAUK www.journals.pan.pl

ARCHIVES OF ELECTRICAL ENGINEERING VOL. 74(1), pp. 227–245 (2025)

DOI 10.24425/aee.2025.153021

Evaluation of the influence of temperature on the parameters of the Jiles–Atherton model and magnetization curves of a 50% Fe–Ni type alloy

WOJCIECH PLUCINSKI[1,2], ZIEMOWIT MALECHA[1], KRZYSZTOF TOMCZUK[1]

[1] *Wrocław University of Science and Technology*
Departament of Cryogenics and Aerospace Engineering
50-370 Wrocław, Poland

[2] *Collins Aerospace*
Bierutowska 65-86, 51-317 Wrocław, Poland

e-mail: {wojciech.plucinski/ziemowit.malecha/krzysztof.tomczuk}@pwr.edu.pl, wojciech.plucinski@collins.com

(Received: 15.11.2024, revised: 10.02.2025)

Abstract: This paper presents an original method for defining the magnetization characteristics of a 50% iron-nickel alloy as functions of ambient temperature. The presented method, based on Jiles–Atherton theory, reduces the cost and time needed to build a multifactor theoretical model of a ferromagnetic material in relation to temperature. The determination of the J-A equation parameters, which are crucial to obtain theoretical magnetization characteristics that are consistent with the real ones, is always challenging due to the imperfection of the J-A model. The authors focused on determining the temperature dependent magnetization characteristics DC in the range of low magnetic field strength. Based on the results of the experiment, the relationships between temperature and parameters of the basic J-A model were determined and discussed. The study was carried out for a wide temperature range often specified for high-performance electrical or electromechanical devices. The data presented and the method described can be successfully used to build Multiphysics models of magnetic phenomena.

Based on the available knowledge, material data for the 50% Fe–Ni alloy, treated without a H_2 reducing atmosphere, has not yet been published in the universal form presented by the authors.

The presented data and relationships between physical quantities were verified and confirmed experimentally. The presented measurement method is consistent with the industry standard IEC 60404-4.

Key words: 50% Fe–Ni, Jiles–Atherton model, magnetic hysteresis, soft magnetic material

© 2025. The Author(s). This is an open-access article distributed under the terms of the Creative Commons Attribution-NonCommercial-NoDerivatives License (CC BY-NC-ND 4.0, https://creativecommons.org/licenses/by-nc-nd/4.0/), which permits use, distribution, and reproduction in any medium, provided that the Article is properly cited, the use is non-commercial, and no modifications or adaptations are made.

www.czasopisma.pan.pl PAN POLSKA AKADEMIA NAUK www.journals.pan.pl

1. Introduction

Owing to global trends and the development of electromobility and automation, the number of devices equipped with electric drives and electromechanical transducers will increase in the coming years [1]. Apart from the introduction of new products, innovative design methods have been developed. With an ever-increasing computing power, most theoretical analyses performed by engineers take the form of Multiphysics studies. The multiphysics theoretical model allows for a much better understanding of the behaviour of developed products under real operating conditions during early concept design phases. However, this approach requires the preparation of an appropriate set of input data, including a multi-dimensional description of a Soft Magnetic Material (SMM). Although many problems can be addressed through numerical studies, the experimental analysis of magnetic components and systems remains indispensable. The influence of boundary conditions on magnetic properties has been the subject of many publications and scientific papers owing to the complexity of this problem [2, 3]. Detailed scientific discussions on magnetic materials and methods can also be found in the literature [3, 4]. Furthermore, the modelling of magnetic hysteresis has been discussed in recent reviews [5]. To complete this knowledge, the authors present an efficient method for the determination of the magnetic properties of a 50% Fe–Ni alloy for Magneto-Thermal finite element method (FEM) analysis.

The 50% Fe–Ni exhibits high saturation induction and permeability. Its high performance level and chemical purity render it particularly suitable for applications requiring high accuracy and sensitivity. Owing to their popularity and optimal magnetic properties, two-phase soft Fe and Ni-based magnetic alloys are often the first choice for designing transducers and high-performance precision actuators [1]. However, data for this material considering non-standard boundary conditions have rarely been published. The novel method proposed in the present study is the determination of the magnetisation characteristics of this alloy using the basic Jiles–Atherton (J-A) model, integrated with a system of linear equations describing the dependence of its parameters as a function of temperature.

An accurate definition of the magnetic properties of materials is crucial for the effective development of theoretical models of magnetism. It should be noted that the catalogue material data published by manufacturers of ferromagnetic alloys refer to the magnetic properties of the material itself and not to the magnetic cores made from it [6]. Furthermore, these data are usually verified under strictly defined test conditions. In practice, in addition to alloy composition, variables such as structure, processing technology, structural stresses, temperature, and other factors, determine the characteristics of the magnetic induction B generated in a magnetic circuit when exposed to an external magnetic field. It is also important to consider the nature and rate of change in magnetic field strength H. Correct assessment of the influence of the boundary conditions on the magnetisation curves is therefore crucial to ensuring the high accuracy of the Multiphysics numerical analyses that have become standard in engineering practice today.

It is a well-established fact that an increase in temperature results in a reduction in saturation magnetisation, a narrowing of the hysteresis loop, an easier process of remagnetisation, and a decrease in hysteresis loop asymmetry. Therefore, it is essential to consider these changes when accurately modelling and simulating the behaviour of ferromagnetic materials under various temperature conditions. It is also worth noting that the influence of temperature on the magnetisation in the classical approach for temperatures well below the transition is often defined using the

www.czasopisma.pan.pl PAN POLSKA AKADEMIA NAUK www.journals.pan.pl

Bloch law's equation. This description is also approximate and refers to the level of technical magnetization. Nevertheless, the authors were interested in the possibility of creating more accurate empirical equations describing the tested material based on the J-A approach, extending this model by temperature-dependent parameters.

Currently, the most commonly used analytical methods for describing domain behaviour in a ferromagnet exposed to a magnetic field are the Stoner–Wohlfarth, Preisach, Chua–Stromsmoe, and J-A models [7, 8]. The latter is particularly recommended as a convenient way of defining input data in theoretical engineering analyses, such as Finite element analysis (FEA). The J-A model is also supported by software developers such as COMSOL, ANSYS, and MathWorks, and it is employed in tools such as MATLAB and Simscape [9].

In light of the criticism surrounding the veracity of the J-A theory as a physical description of the magnetic hysteresis loop, the authors employed the five parameters J-A model primarily as a mathematical instrument to replicate the trajectory of the hysteresis loop and initial magnetisation curve obtained from the measurement under quasi-static excitation conditions.

Despite the imperfections of the J-A theory, the simplicity of the model's notation and its status as one of common tools for materials characterization in commercial engineering simulation programs were key considerations in its selection. The authors approach, which involves the definition of an empirical formula based on mathematical assumptions inherent to the basic J-A equation and the adjustment of parameters in function of variable temperature.

This paper presents an evaluation of the influence of temperature, ranging from –55 to 195°C. The objective of the research was to apply the obtained results to Multiphysics analyses of electrohydraulic valve used in aviation applications. Consequently, the lower temperature limit was defined as a rational minimum operating temperature for aviation equipment installed in airframe zones where temperature control is not required. The upper limit was assumed, taking into account the temperature limitations of organic insulating materials for long-term service.

In the case of polyimide-based insulation, the continuous operating temperature should not exceed approximately 200°C. In the context of aviation applications, such temperatures may be specified for low-power electromechanical devices installed, for example, as aircraft engine accessories. It is also important to note that, in contrast to power applications, these devices (solenoids, torquemotors) often process a signal in the form of direct current. Furthermore, as demonstrated by S.E. Zirka *et al.* [10]. the popular Jiles–Atherton model better reflects the shape of static than dynamic hysteresis. Consequently, the authors have a particular interest in DC and quasi-static magnetisation characteristics. Nevertheless, the DC magnetisation characteristic is frequently employed as a basis for the construction of magnetisation curves for cores subjected to an alternating current problems.

In addition to discussing the measurement data, this article presents the post-processing method that allows the development of a parameterised theoretical model of the soft magnet based on the processing of a recorded hysteresis loop. The proposed algorithm allows the scaling of the $B(H)$ hysteresis loops, obtained from measurements performed in accordance with method A as per the standard [11], to static DC curves determined at multiple points in accordance with method B. Using examples of measurements and analyses, arguments for and against the use of the J-A model and multi-dimensional linear interpolation lookup tables to describe the magnetic properties of SM materials have been discussed [12].

www.czasopisma.pan.pl PAN POLSKA AKADEMIA NAUK www.journals.pan.pl

2. Materials and method

2.1. Theoretical model of the material

To describe the theoretical relationship $B(H,T)$ for the case presented in this study, the magnetisation characteristics were noted as a function of temperature using the J-A five parameters basic model (3).

The theoretical bases of the J-A model are the theories of Weiss and Langevin. The J-A model is based on an anhysteretic magnetisation curve [13]. For isotropic materials, the anhysteresis magnetisation curve is determined using the Langevin curve.

$$M_{\mathrm{ah}} = M_{\mathrm{s}} \left[\coth\left(\frac{H_{\mathrm{eff}}}{a}\right) - \frac{a}{H_{\mathrm{eff}}} \right], \tag{1}$$

where M_{s} is the magnetisation saturation state, a describes the domain-wall density, and H_{eff} is the effective field strength. This equation can be compared with the Bloch model, which describes the relationship between the external magnetic field H, total magnetisation M, and inter-domain coupling α. According to the Bloch model [7],

$$M_{\mathrm{eff}} = H + \alpha M. \tag{2}$$

In the J-A model, M is determined by the following differential equation:

$$\frac{\mathrm{d}M}{\mathrm{d}H} = \frac{\delta_{\mathrm{M}}}{(1+c)} \frac{(M_{\mathrm{ah}} - M)}{(\delta k - \alpha(M_{\mathrm{ah}} - M))} + \frac{c}{(1+c)} \frac{\mathrm{d}M_{\mathrm{ah}}}{\mathrm{d}H}, \tag{3}$$

where c is the parameter that determines the reversibility of the magnetisation, δ is equal to 1 for an increasing magnetic field H and–1 for a decreasing one, and δ_M accounts for the unphysical case in which the gain in magnetic permeability $\mathrm{d}B/\mathrm{d}H$ becomes negative. The latter δ_M is zero in two cases: when $(M_{\mathrm{ah}} - M) > 0$ for a decreasing magnetic field strength H and when $(M_{\mathrm{ah}} - M) < 0$ for an increasing field strength H. In the other cases δ_M is equal to 1 and negligible. It is noteworthy that the exact solution of (3) requires the use of a fourth-order Runge–Kutta algorithm. The above-mentioned theory and the MATLAB/Octave script for solving the corresponding equations have been reported previously [8].

As pointed out by some researchers [10, 14], the Jiles–Atherton theory cannot be interpreted as the perfect physic-basis description. Nevertheless, the fundamental concept, based on the J-A theory, is widely used by commercial software developers as one of the methods for defining the magnetic properties of a material. It also reasonable to assume that the ambient temperature has a significant impact on multiple parameters of the J-A model, which consequently affects the magnetic characteristics of the described ferromagnet.

2.2. Material tested

The nonoriented SMM 50%Fe–Ni [15] was subjected to magnetic annealing, a heat treatment process. The process was carried out without a reducing atmosphere H_2 in a vacuum furnace. The temperature and annealing time were set to 1170°C, 4 h, respectively; these parameters were defined in accordance with industry guidelines [6]. The aim of the magnetic annealing process was

to obtain a structure and grain size (approx. 0.7 [mm]), that would allow a minor reduction in the relative permeability μ_r in the intermediate magnetisation range, with a minimum reduction in the induction value for the technical saturation state, compared with the maximum magnetic parameters of the alloy as defined by the steelworks (up to 95%). In practice, obtaining an optimum value for μ_r has a positive effect on the electro-mechanical characteristics of an analogue transducer such as an electro valve. This reduces the sensitivity of the Electro-Mechanical Interface Device to low-amplitude current noise which can act as the background for the control signal of this device. The $B(H,T)$ measurements were carried out on ring samples with a solid cross-section and the following dimensions: outer diameter D:36 [mm], inner diameter d:30 [mm], and width z:5 [mm]. The excitation winding (20 turns) and measuring winding (60 turns) were made of polyimide-insulated wire. The magnetic properties $B(H,T)$ were measured in 10 representative samples.

In addition, to facilitate the verification of the data processing method used, specimens made of Fe20%–Ni80% (material in accordance with Alloy 4 composition as per [15]) with the same geometry and winding configuration were tested. The $B(H)$ characteristics of mumetal, previously described by the J-A model, were used as a reference. The permalloy J-A parameters have been reported [8]; however, the temperature factor was omitted.

The tested material exhibited an optimal grain size (0.5÷0.8 [mm]), which is crucial for achieving the high magnetic permeability and low coercivity. The presence of smaller grains (structure before annealing. Fig. 1(a)) increases the number of grain boundaries, which in turn impedes the movement of domain walls and consequently reduces the permeability of the material. The presence of larger grains (Fig. 1(b)) results in a reduction in the density of grain boundaries, thereby facilitating the movement of domain walls and consequently increasing permeability. In order to ascertain the grain size of the tested ring specimens, the surfaces of the tested ring specimens were polished several times with polishing cloths containing a diamond suspension using a metallographic polisher. The specimen surface was etched with an aqueous solution of nitric and hydrochloric acid. The revealed microstructures of samples material before and after magnetic annealing, observed with a Keyence®VHX 2000 microscope, are shown in figure below.

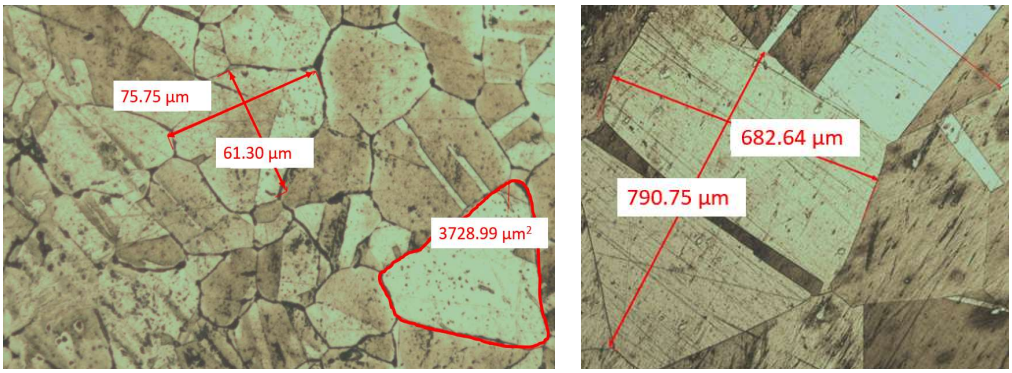

(a) (b)

Fig. 1. Comparison of the crystal structure in the tested material before (a) and after (b) magnetic heat treatment

2.3. Test stand

Magnetic loops were recorded using a purpose-built modular measurement system; the resulting block diagram is shown in Fig. 2. An unusual novel solution employed in the present study was using a current source, SMU2450 (Keithley, UK), to generate arbitrary magnetising current waveforms. The use of a PC-controlled power supply via an algorithm defined in the LABview®environment eliminates the influence of the human factor on measurements. An additional resistor was connected in series in the excitation circuit to ensure the stability of the control loop within the SMU. An EF5 electronic fluxmeter (Magnet-Physik, Germany) was used to measure the induced magnetic flux. The prepared samples were placed in a climatic chamber. The magnetising current was converted into a voltage signal at the measuring resistor and an analogue voltage signal 0–10 [Vdc] proportional to the magnetic flux from the electronic fluxmeter output was recorded using a multichannel data acquisition system (Dewetron, US).

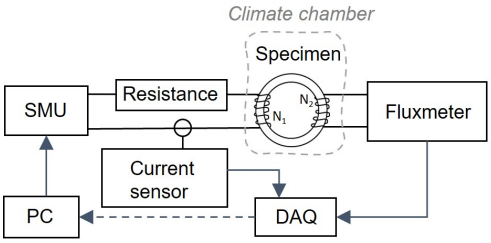

Fig. 2. Schematic diagram of the measurement system used

2.4. Method of measurement

The $B(H,T)$ relationship was measured according to industry standards [11]. The continuous method A was used; the magnetic flux was measured with a monotonically increasing/decreasing magnetic field strength in the core sample. The authors elected to employ the quasi-static measurement method, which simulates the working conditions of the magnetic core in micro-actuators that are controlled by a continuous current signal. The rate of change of the field strength was $\mathrm{d}H/\mathrm{d}t = 5$ [A/(m·s)]. Continuous measurements reduced the influence of the possible drift of the fluxmeter display on the test results and their subsequent interpretation. The measurements were performed in the automatic mode and test data were recorded in the time domain at a sampling rate of 1 [kHz]. As shown below, each magnetisation cycle was preceded by a demagnetisation procedure using a sinusoidal waveform current signal with a periodically decreasing amplitude (Figs. 3(a), 3(b)). The recorded test data were processed in MATLAB 2020a.

Additionally, a moving-average filter was used to smooth noisy data. This solved the noise problem caused by the digital source of the excitation signals. The following difference equation describes the moving average filter used:

$$y(n) = \frac{1}{\mathrm{ws}} \left(x(n) + x(n-1) + \ldots + x(n-(\mathrm{ws}-1)) \right), \tag{4}$$

where, ws (window size) was set to 80 records.

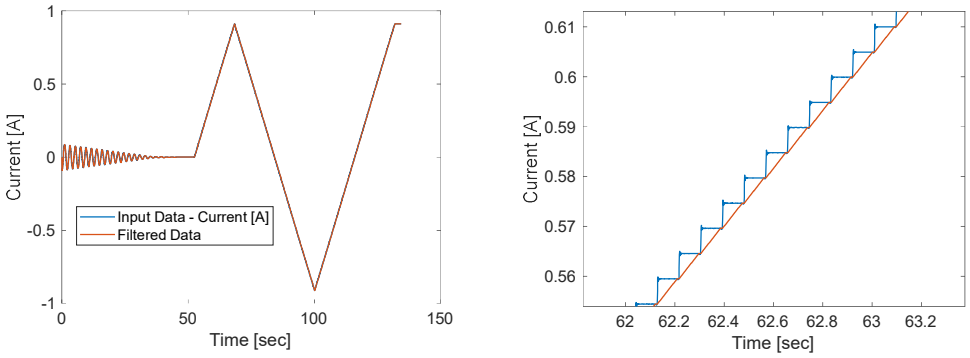

Fig. 3. Magnetizing current in the excitation coil: (a) real excitation and filtered in post processing; (b) zoomed view

The values of magnetic induction B and magnetic field strength H in the considered specimen magnetic circuit were obtained based on the following assumptions:

$$H = \frac{N_1 \cdot I}{l}, \tag{5}$$

where H is the magnetic field strength, N_1 is the number of excitation coil turns, I is the current in the primary winding, and$l$ is the magnetic core length.

$$\Delta B = \frac{K_\mathrm{B} \cdot \alpha_\mathrm{B}}{N_2 \cdot A}, \tag{6}$$

where B is the magnetic induction, α_B is the fluxmeter reading, K_B is the fluxmeter constant, N_2 is the number of measuring coil turns, and A is cross-sectional area of the sample.

Based on these equations, it is possible to plot the $B = f(H,T)$ relationship. However, data in this form (hysteresis loop) may not be sufficient as input for theoretical Multiphysics models in tools such as Simscape, COMSOL, and ABAQUS. Therefore, converting the determined vectors B and H in relation to T into a parametric description using the J-A method was proposed. The measurement algorithm proposed is shown in Fig. 4.

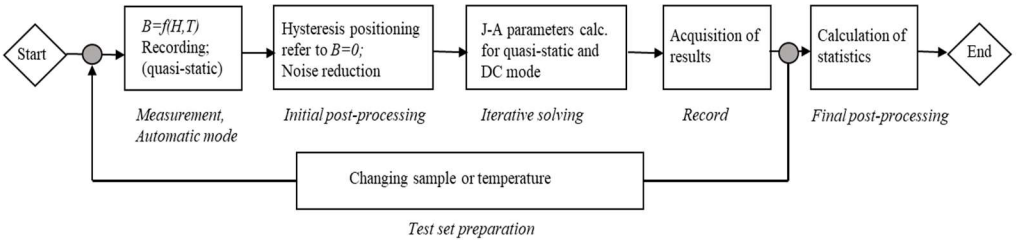

Fig. 4. Schematic diagram of the measurement algorithm used

The results are presented in Figs. 5, 7. The blue curves, which are the measurement records, were used to plot the anhysteretic curves, which are the basis for the J-A model, and to determine the values of coercivity *Hc* and remanence *Br*. Based on these data, the parameter values of the theoretical J-A models that fit the actual hysteresis loop were selected using an iterative simplex method. The $B(H)$ loop reproduced by the J-A model was transformed into a static DC characteristic. For this purpose, the magnetisation characteristics measured at 30°C were compared with the hysteresis loop measured at RT conditions, using the point-to-point method in accordance with [11] (dashed pink line, Fig. 5). This allowed us to establish a relationship between the parameter k in the J-A equation and the magnetic field strength per time derivative. The coefficient k effectively describes the magnetic losses. As shown in [2, 8, 14], the J-A method also allows for the accurate reconstruction of the primary magnetisation curve, the shape of which is difficult to determine for SM materials.

3. Results

This section presents the magnetisation characteristics of the tested alloy determined at selected temperatures – assumed as typical operating conditions for electromagnetic devices classified as avionics sensors and aircraft actuators. Measurements at defined operating points formed the basis for the development of the parametric J-A model, which is also presented and discussed.

Both the measured characteristics and the reconstructed curves are presented below (Fig. 6).

The obtained theoretical curves (orange solid line, Fig. 5), which coincide with the real state (Fig. 5), can be successfully used as a universal definition of the magnetic properties of the

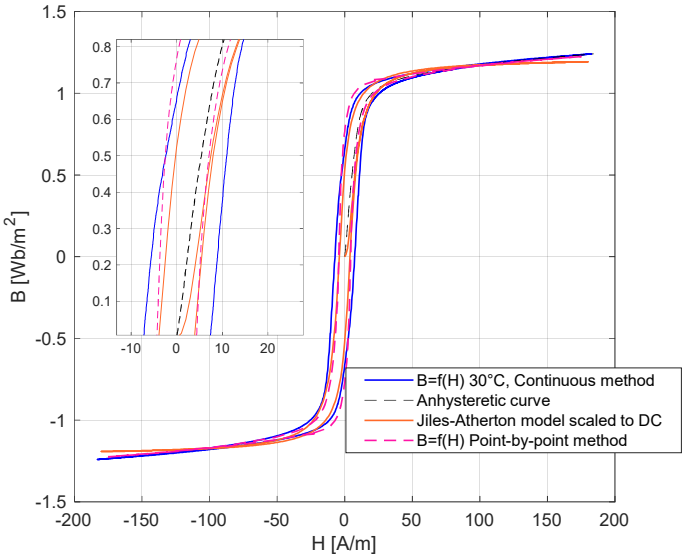

Fig. 5. Magnetisation characteristics – model vs measured at 30°C

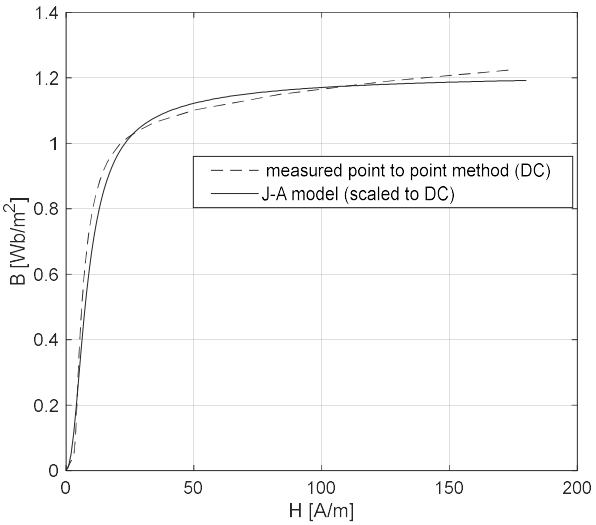

Fig. 6. Comparison of initial magnetisation curves – model vs measured at 30°C

ferromagnet in numerical analysis (FEM). An example of a comparison between the reconstructed initial magnetisation curve and that measured under RT conditions using method *B* in accordance with standard [11] is shown in the plot below.

For example, the measured magnetisation characteristics are $B(H,T)$ at low temperatures. Boundary conditions and their theoretical model equivalents are shown in Fig. 7.

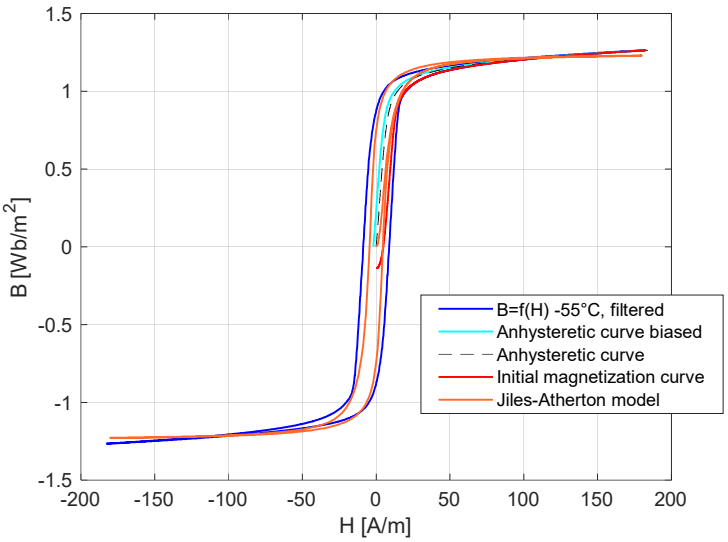

Fig. 7. Magnetisation characteristics – model vs measured at –55°C

To better illustrate the influence of temperature on the selected magnetisation curves, summaries of the measured hysteresis loops are also plotted (Fig. 8).

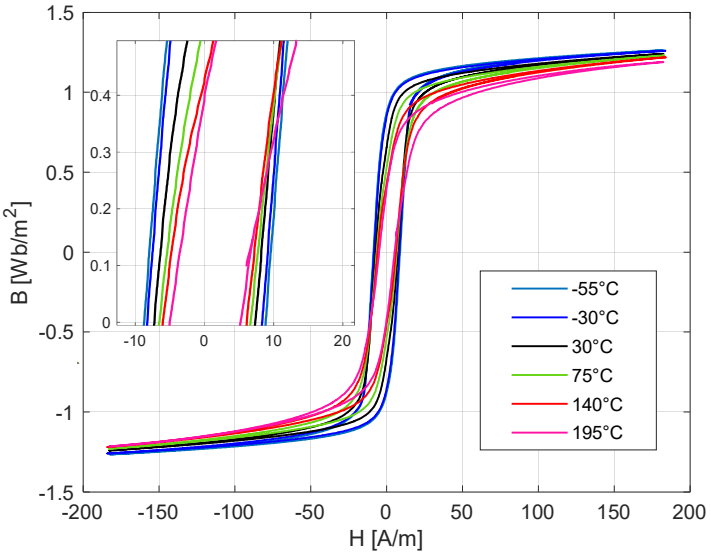

Fig. 8. Magnetisation characteristics measured in the temperature range of –55°C to 195°C

A summary of the theoretical magnetisation hysteresis loops reconstructed and scaled to the DC state using the J-A method is presented below (Fig. 9). Initial magnetisation curves are shown in Fig. 10.

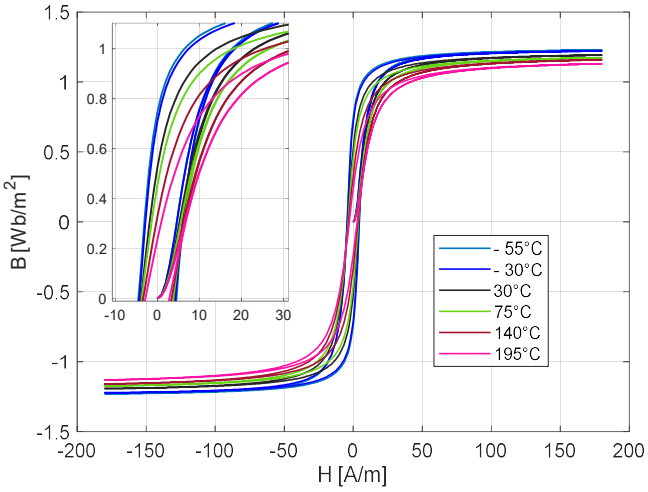

Fig. 9. Magnetisation characteristics as per J-A model in the temperature range of –55 to 195°C

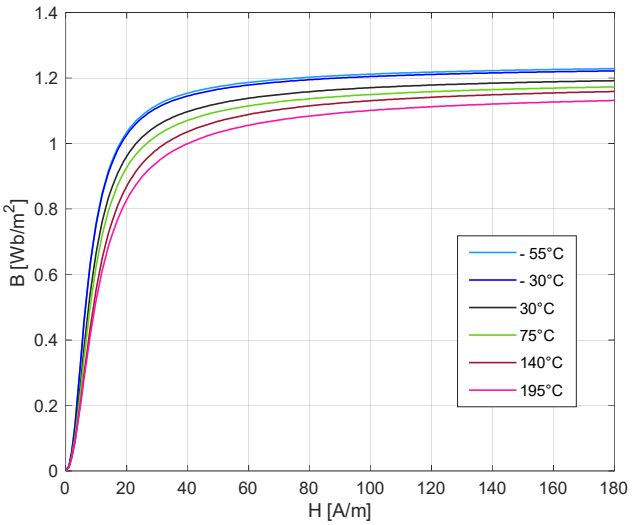

Fig. 10. Initial magnetisation curves as per the J-A model in the temperature range of –55 to 195°C

The experimentally determined J-A model parameters are listed in Table 1; these parameters should be interpreted as follows: M_s, saturation magnetisation of the material; a, domain wall density; α, Bloch interdomain coupling; k, average energy required to break the pinning site; and c, magnetisation reversibility [8].

Table 1. J-A parameters summary (average values)

T **[°C]**	**J-A model parameters**				
	a **[A/m]**	***k*** **[A/m]**	***c***	$\boldsymbol{M_S}$ **[A/m]**	α
–55	3.030	5.040	$4{\cdot}10^{-5}$	$9.94{\cdot}10^{5}$	$6{\cdot}10^{-6}$
–30	3.151	4.788	$4{\cdot}10^{-5}$	$9.89{\cdot}10^{5}$	$6{\cdot}10^{-6}$
30	4.040	4.200	$4{\cdot}10^{-5}$	$9.70{\cdot}10^{5}$	$6{\cdot}10^{-6}$
75	4.444	3.990	$4{\cdot}10^{-5}$	$9.57{\cdot}10^{5}$	$6{\cdot}10^{-6}$
140	5.454	3.497	$4{\cdot}10^{-5}$	$9.51{\cdot}10^{5}$	$6{\cdot}10^{-6}$
195	6.060	2.940	$4{\cdot}10^{-5}$	$9.31{\cdot}10^{5}$	$6{\cdot}10^{-6}$

For the cases studied, the effect of (T [°C]) can be reproduced using 3 of the 5 parameters of the basic J-A model; these parameters being: $\boldsymbol{a}$, $\boldsymbol{k}$, M_s. The constants $\boldsymbol{c}$ and α remain statistically unchanged or variation was lower than the measurement system sensitivity.

www.czasopisma.pan.pl PAN POLSKA AKADEMIA NAUK www.journals.pan.pl

The aforementioned conclusions were reached through the statistical processing of research results. As a consequence of the measurements, normal distributions were obtained for all J-A parameters at studied operating points. Levene's test was also conducted to verify the homogeneity of variances for parameter values. However, the importance of the influence of the temperature on the individual J-A model parameters was assessed on the basis of the probability plots presented below (Fig. 11–15). The static tests were further augmented by the Mood's median test.

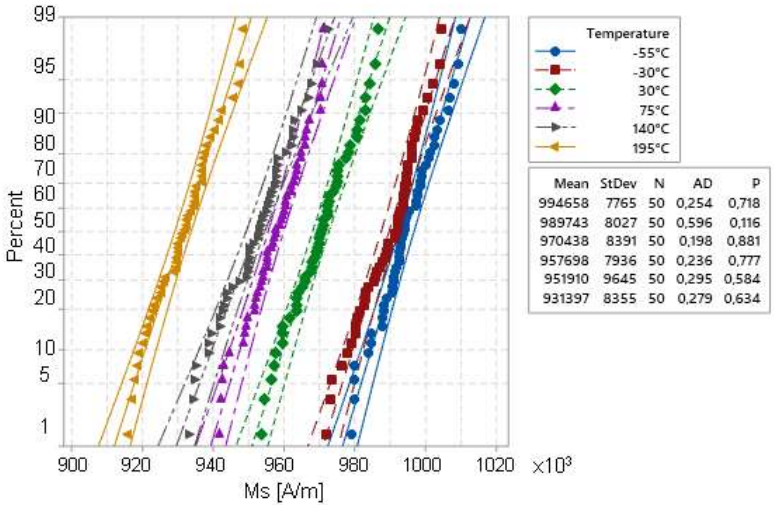

Fig. 11. Probability plot comparing the distributions of parameter M_s in temperature range of –55 to 195°C

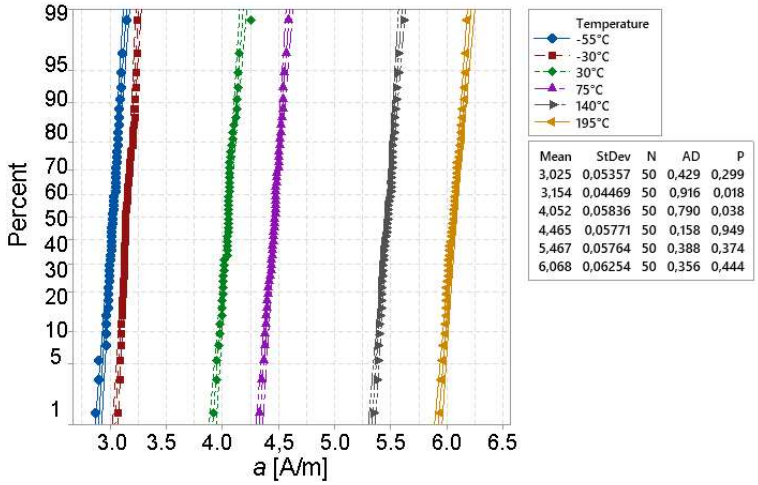

Fig. 12. Probability plot, the distributions of parameter a in temperature range of –55 to 195°C

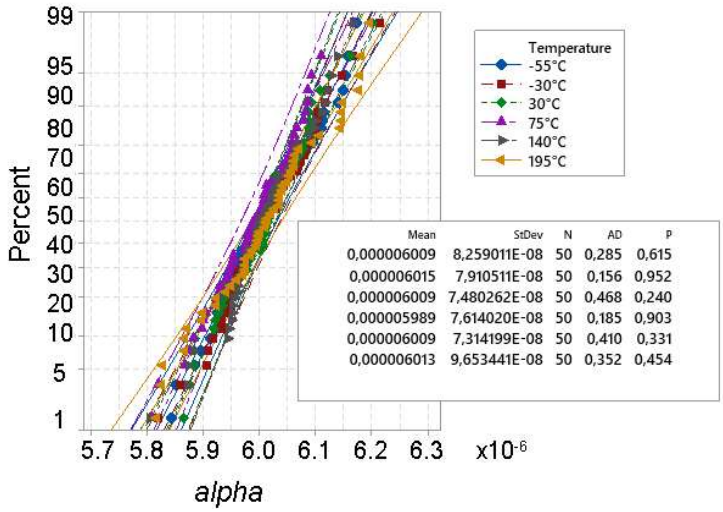

Fig. 13. Probability plot, the distributions of parameter α in temperature range of –55 to 195°C

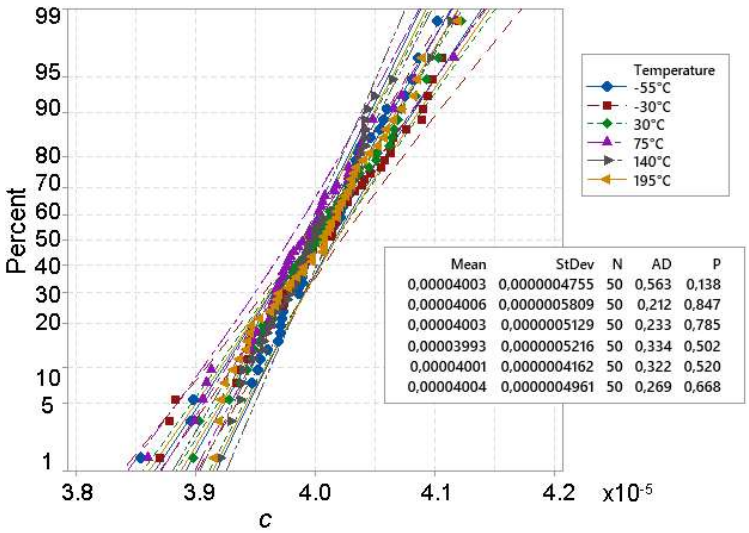

Fig. 14. Probability plot, the distributions of parameter c in temperature range of –55 to 195°C

In addition, a linear range of ±0.05 [T] was found for the measured anhysteretic curves (Fig. 16). It is worth noting that these characteristics largely coincide with the initial 'magnetisation curve determined by Method B in accordance with [11] (in the present experiment, the value of *Hc* for continuous measurements was approximately 2 *Hc* DC).

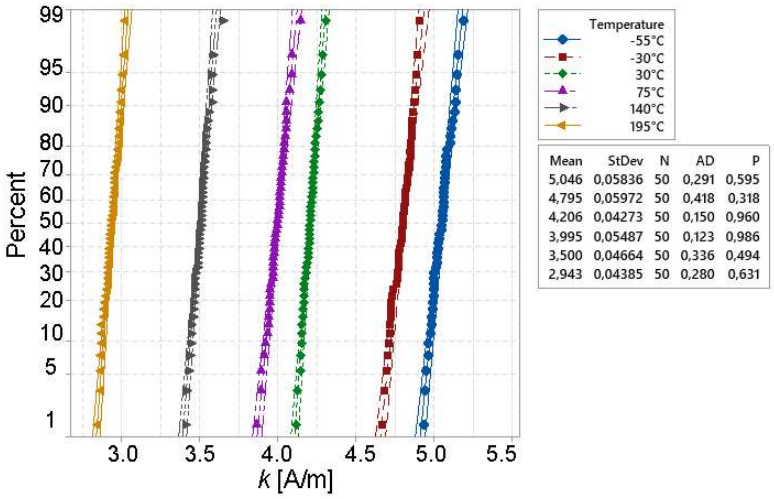

Fig. 15. Probability plot, the distributions of parameter k in the temperature range of –55 to 195°C

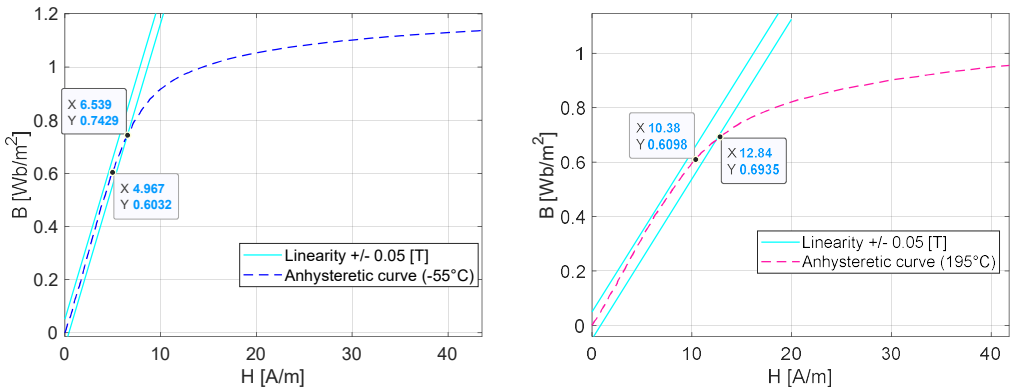

(a) (b)

Fig. 16. Anhysteretic magnetisation curves measured at low (a) and high (b) temperatures

4. Discussion

Based on the test data and analysis performed, we conclude that the ambient temperature variation has a significant effect on both the change in the relative magnetic permeability μ_r and the level of magnetisation for the technical saturation state. The value of the coercive force Hc also changed as a function of temperature, which manifested as an increase in the loss of the core operating at low temperatures (Table 2). As the temperature increases, the quasi-linear range of $B(H)$ decreases.

For the cases discussed, a temperature variation from –55 to 195° C resulted in a change in the magnetic induction value of approximately 6% (from 1.263 [T] to 1.189 [T]) for a magnetic field strength of 182 [A/m]. The ambient temperature variation had an even greater effect on the

Table 2. Coercivity values for different temperatures and measurement methods

Fe–Ni alloy per ASTM A753 alloy type 2			
T **[°C]**	***Hc*** **[A/m] for** $\mathbf{d}H/\mathbf{d}t$ **= 5 [A/ms]**	***Hc*** **[%] in ref. to value at 30°C**	***Hc*** **[A/m] scaled to DC method**
–55	8.78	120.5	3.86
–30	8.30	113.9	3.65
30	**7.29**	**100.0**	3.21
75	6.60	90.5	2.90
140	6.07	83.3	2.67
195	5.11	70.1	2.25

coercive force Hc values. The changes ranged from approximately 70 to 120% of the reference value of 3.21 [A/m] ± 0.2 [A/m], determined at 30°C. The results are summarised in Table 2.

As mentioned above, the J-A method is the preferred method for describing the magnetic characteristics of the inductive components in FEM modelling or MATLAB simulations. However, a disadvantage of the basic J-A model is its limited ability to represent the shape of the magnetisation curve in the paraprocess region [3]. This is particularly evident in the $B(H,T)$ curves which were recorded at high temperatures. The problem of reproducing the full magnetisation curve can be solved using array definitions, such as lookup tables. Linear interpolation is the simplest and most efficient method for preparing material data for engineering analysis; however, it is not suitable if the initial magnetisation curve needs to be reconstructed based on the measured hysteresis loop or if the modelled magnetisation curve is dynamic. The use of arrays is also not an optimal solution if the material being described exhibits strongly nonlinear behaviour as a function of temperature. Such an example would be the mumetal (ASTM A753 Type 4 alloy) where, as shown in the diagram below (Fig. 17), the magnetic permeability vector changes its direction once the temperature exceeds approximately –30°C. Neural network-based models can be used as alternative tools for approximating hysteresis loops. This approach does not require knowledge of the modelled phenomenon, it only requires importing the learning data [16].

In contrast to the lookup table, the J-A model, which is based on physical description, can be interpolated or extrapolated to other cases, which is an advantage. The linear functions used to determine the values of the J-A–parameters as functions of temperature for the boundary conditions defined in this study using regression method (Fig. 18) are as follows:

$$\begin{cases} a = 0.01253T + 3.622 \\ k = 80.62 \cdot 10^{-4}T + 4.553 \\ M_{\mathrm{s}} = -243.7T + 9.798 \cdot 10^{5} \\ \alpha = 6 \cdot 10^{-6} \\ c = 4 \cdot 10^{-5} \end{cases}, \tag{7}$$

where T is the temperature in degrees Celsius.

www.czasopisma.pan.pl PAN POLSKA AKADEMIA NAUK www.journals.pan.pl

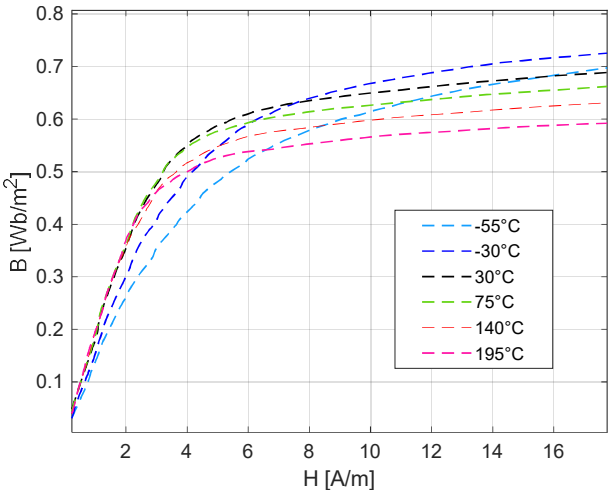

Fig. 17. Anhysteretic magnetisation curves of the ASTM A753 Alloy 4, measured in the temperature range of –55 to 195°C

In practice, for the analysed case, by defining the J-A model parameters based on three linear functions (7), any number of magnetisation DC hysteresis loops and initial magnetisation curves can be generated for the temperature range studied.

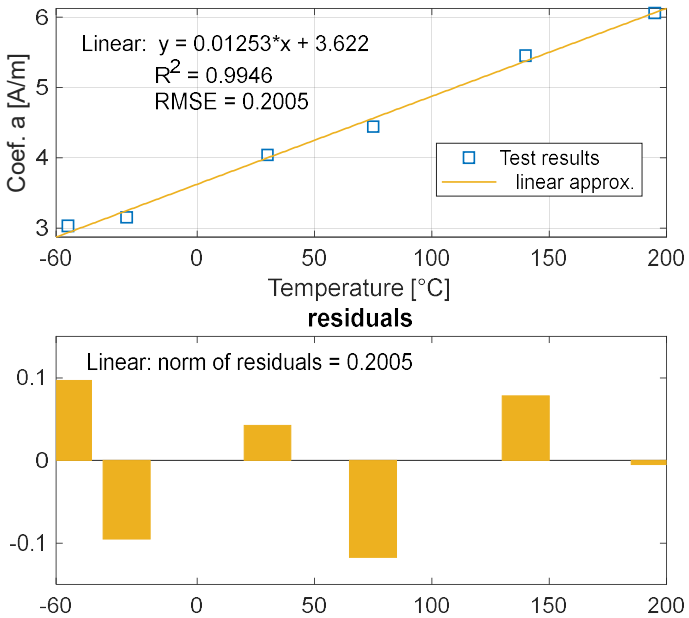

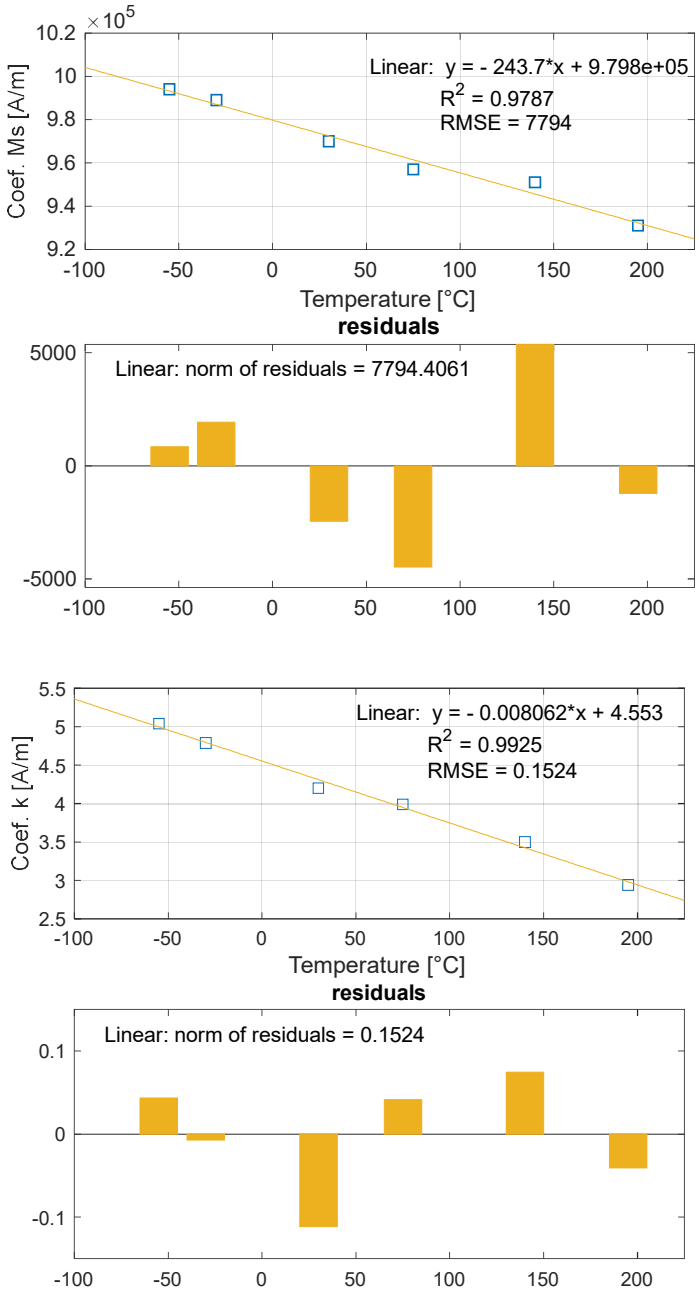

Fig. 18. Linear approximation of the J-A model parameter values for the ASTM A753 Alloy 2 in the temperature range of –55 to 195°C

www.czasopisma.pan.pl PAN POLSKA AKADEMIA NAUK www.journals.pan.pl

5. Conclusions

The results of the measurements and subsequent analysis indicate that the use of the basic Jiles–Atherton model as a mathematical apparatus and the modification of its parameters based on specific empirical relationships presented in the form of a linear function represents a convenient method of defining magnetisation curves for studied cases. The imperfection of the J-A theory as a representation of the physical phenomenon of magnetisation has been mitigated. Moreover, the impact of temperature on the trajectory of magnetisation curves was delineated with greater accuracy than in the case of the using Bloch's law equation. Temperature affects the parameters of the Jiles–Atherton. Generally, increasing temperature leads to reduced saturation magnetization, narrower hysteresis loops, easier remagnetisation.

The effect of temperature on the $B(H)$ characteristics of the tested SMM for studied cases can be reproduced by the basic J-A model using only three of its five parameters: a, k, and M_s. It is important to note that the model parameters should be considered simultaneously. The effect of temperature on the $B(H)$ characteristics for the conditions described in this paper is significant. Therefore, the influence of temperature should not be ignored when designing mechatronic devices operating under harsh conditions; these devices may also include aerospace accessories. It should be noted that in the studied temperature range considered for 50% iron-nickel alloy, the changes in the J-A parameters can be represented by linear functions.

The presented research results are applicable to Multiphysics FEA-based theoretical models developed for electromechanical transducers. This study focuses on the development of effective methods for designing mechatronic components intended to function under extreme environmental conditions. Presented approximation to be fully satisfactory for engineering applications. Moreover, presented model can be readily expanded in the future to incorporate the influence of additional factors, such as excitation frequency and the impact of mechanical stresses. In the future, a similar empirical model could be employed to describe novel materials with unconventional structures, such as those produced using the additive methods.

References

[1] Waeckerlé T., Perichon P., Ateba-Betanda Y., Demier A., *Recent progress in the application development of Fe50Ni50 type alloys*, Journal of Magnetism and Magnetic Materials, vol. 564, Part 1 (2022), DOI: 10.1016/j.jmmm.2022.170075.

[2] Chwastek K., *Parametric examination of a phenomenological model of ferromagnetic hysteresis*, Prace Instytutu Elektrotechniki (in Polish), vol. 252, pp. 41–54 (2011).

[3] Cullity B.D., Graham C.D., *Introduction to magnetic materials*, John Wiley & Sons, Inc., Hoboken, New Jersey, ISBN: 978-0-471-47741-9 (2009).

[4] Zijlstra H., *Experimental Methods in Magnetism*, North-Holland, Amsterdam, vol. 2 (1967).

[5] Mörée G., Leijon M., *Review of Hysteresis Models for Magnetic Materials*, Energies, vol. 16, iss. 9 (2023), DOI: 10.3390/en16093908.

[6] https://www.carpenterelectrification.com/resources, accessed February 2024.

[7] Jiles D.C., Atherton D.L., *Theory of ferromagnetic hysteresis*, Journal of Applied Physics, vol. 55, pp. 2115–2121 (1984), DOI: 10.1063/1.333582.

[8] Szewczyk R., *The method of moments in Jiles–Atherton model based magnetostatic modelling of thin layers*, Archives of Electrical Engineering vol. 67, no. 1, pp. 27–35 (2018), DOI: 10.24425/118989.

www.czasopisma.pan.pl PAN POLSKA AKADEMIA NAUK www.journals.pan.pl

[9] www.mathworks.com/help/sps/ref/nonlinearreluctance.html, accessed February 2024.

[10] Zirka S.E., Moroz Y.I., Harrison R.G., Chwastek K., *On physical aspects of the Jiles–Atherton hysteresis models*, Journal of Applied Physics, vol. 112, 043916 (2012), DOI: 10.1063/1.4747915.

[11] IEC 60404-4, *Methods of measurement of d.c. magnetic properties of magnetically soft materials*, Edition 2.2 (2008).

[12] www.mathworks.com/help/simulink/lookup-tables.html, accessed February 2024.

[13] Jiles D.C., Atherton D.L., *Theory of ferromagnetic hysteresis*, Journal of Magnetism and Magnetic Materials, vol. 61, pp. 48–60 (1986), DOI: 10.1016/0304-8853(86)90066-1.

[14] Szewczyk R., *Computational problems connected with Jiles–Atherton model of magnetic hysteresis, Advances in Intelligent Systems and Computing*, Springer, vol. 267, pp. 275–283 (2014).

[15] ASTM International, *Standard Specification for Wrought Nickel-Iron Soft Magnetic Alloys (UNS K94490, K94840, N14076, N14080)*, A753 (2021).

[16] Dudek G., *Approximation of the hysteresis loop using computational intelligence methods*, Przegląd Elektrotechniczny (in Polish), ISSN 0033-2097, R. 88, vol. 88, no. 12, pp. 8–11 (2012).